



Analysis of Velocities, Density and Seismic Facies of Ariri Formation – Santos Basin.

Thiago Yamamoto (Petrobras, UFF); Alexandre Maul (Petrobras, UFF) & Wagner Lupinacci (UFF)

Copyright 2019, SBGf - Sociedade Brasileira de Geofísica

This paper was prepared for presentation during the 16th International Congress of the Brazilian Geophysical Society held in Rio de Janeiro, Brazil, 19-22 August 2019.

Contents of this paper were reviewed by the Technical Committee of the 16th International Congress of the Brazilian Geophysical Society and do not necessarily represent any position of the SBGf, its officers or members. Electronic reproduction or storage of any part of this paper for commercial purposes without the written consent of the Brazilian Geophysical Society is prohibited.

Abstract

The Santos Basin is located in the South Atlantic Ocean and is limited in the north by the Cabo Frio High and in the south by Florianópolis High. It has an area of about 350 thousand km² distributed along the coasts of the states of Rio de Janeiro, São Paulo, Paraná and Santa Catarina. The Santos Basin originated from geological processes that culminated with breakup of the Gondwana Supercontinent during the Cretaceous.

In this basin occurred the deposition of salt sequence during the Aptian Age denominated Ariri Formation. Its sedimentation took place during the transition between the sag and marine phases, under an arid climate associated with periodic marine transgressions. The evaporitic section has thickness varying from few meters up to three kilometers and serves as seal of the reservoirs of the Santos Basin.

The Ariri Formation presents high geological complexity, observable in seismic images and drilled wells. Among the minerals present, we can mention halite, anhydrite, gypsum, tachyhydrite, sylvite, carnalite, volcanic, calcite and others.

Characterizing the properties of salts has great importance for several disciplines related to the oil and gas industry, such as geomechanical modeling, velocity models building, geological forecasting for wells.

Introduction

The Ariri Formation is a Cretaceous/ Neoaptian salt sequence, located in the Santos Basin and deposited in a restricted marine transitional post-rift environment with high evaporation rate. This formation presents a high structural complexity like salt walls, diapirs, pillows and mini basins. The geologic process that form these structures may related to halocinetic forces and extensional process (Gamboa *et al.*, 2008).

Halite is the most common facies in Ariri Formation with proportion ranging from 80 to 90% (Gamboa *et al.* 2008, Amaral *et al.*, 2015, Yamamoto *et al.*, 2016). Others salts such as tachyhydrite, carnalite, sylvite, anhydrite and gypsum, occur in small proportions intercalated with halite, forming the so-called cycles.

Mohriak *et al.* (2008) defines that each primary cycle is marked on base by shales layers rich in organic matter. The evaporites precipitation follows a deposition order dependent on two factors: the solubility and the amount of ions dissolved in brine.

Sonnenfeld (1984) studied the precipitation sequence of evaporitic minerals. The author identified that carbonate minerals (dolomite, calcite) are the first to deposit. Followed by sulfates (gypsum and anhydrite) and halite. Finally, when we have low water available in the system, deposits the soluble minerals like sylvite, carnalite, tachyhydrite and others.

Mavko *et al.* 2009 and Crain 2015 made elastic properties measurement on main evaporitic minerals. From table 01 it is possible to see the values measured by these authors and the relation with degree of evaporite solubility. With the increasing of the mineral solubility, the velocity decrease.

Mineral	Chemical Composition	Mineral Class	Velocity (m/s)
Dolomite	CaMg(CO ₃) ₂	Carbonates	6930-7340 *
Calcite	CaCO ₃	Carbonates	6260-6640 *
Anhydrite	CaSO ₄	Sulfates	5640-6010 *
Gypsum	CaSO ₄ .2H ₂ O	Sulfates	5800 *
Halite	NaCl	Chlorides	4500-4550 *
Sylvite	KCl	Chlorides	4119 **
Carnallite	KMgCl ₃ * 6H ₂ O	Chlorides	3908 **
Tachyhydrite	CaMg ₂ Cl ₆ ·12H ₂ O	Chlorides	3313 **

Table 01: Main evaporitic minerals with respective chemical form, mineral class and velocity value. * Mavko *et al.* (2009), ** Crain (2015)

Maul *et al.* (2018) presented a review of the main techniques used in evaporitic characterization, such as electric logs, seismic, attributes and model-based inversion studies. The authors also commented the importance of Ariri Formation characterization for areas such as geomechanics, seismic processing, well drilling and reservoir studies.

In this study, we will discuss the Ariri Formation characterization for a portion inside the Santos Basin. The work is based on information of electrical logs, facies, seismic and velocity model. We will also comment the seismic limitations in conjunction with the well information.

Method

The present study aimed to characterize the salts present in a portion of the Santos Basin, using well and seismic data. The study area is located on the central portion of

the Santos Basin occupying 95km² on the coast of São Paulo State. The data were delivered by Agência Nacional do Petróleo (ANP) and consists of a depth migrated seismic volume, velocity model used in this data migration and ten well information containing density, gamma rays, sonic P (compressional) and S (shear), porosity and facies curves.

Part of the study is based on the methodology proposed by Amaral *et al.* (2015) to use sample cuttings to complement the acquisition log gaps. The way to perform the analysis was later confirmed by Yamamoto *et al.* (2016) and Cornelius & Castagna (2018). In the mentioned works, the authors estimated salts proportions through facies curves described during the well drilling phase. The facies description is performed under rock fragments crushed by the bit. These descriptions are subject to errors, such as interpretation, sample depth or even operational problems. Another difficulty is related to minerals mixtures that are not represented in descriptions.

We calculated the P and S velocities from the sonic logs and with facies curves, it was possible to separate salts into three groups based on the velocity behavior. Then we estimate the proportion of each facies group.

- 1) Halite, that corresponds to the most common lithology in evaporitic section;
- 2) High-velocities salts (HVS): represented by anhydrite and gypsum which have higher velocities than halite;
- 3) Low-velocity salts (LVS): tachyhydrite, carnalite, sylvite etc, whose velocities are smaller than halite.

We use the density curves, P and S velocities to characterize the elastic properties of evaporites. All the wells have information of compressional waves (figure 01) however due to operational limitations most of them did not have acquired log at the top of Ariri Formation. The S sonic log was acquired in five wells and density in only one.

From P-velocities, we calculate the average, median and standard deviation for each facies. Due to poor information availability, it was not possible estimate the salts densities and S-velocities statistics. However, we have to complete the non-acquired curves because this information is important to well-to-seismic tying and seismic inversion studies.

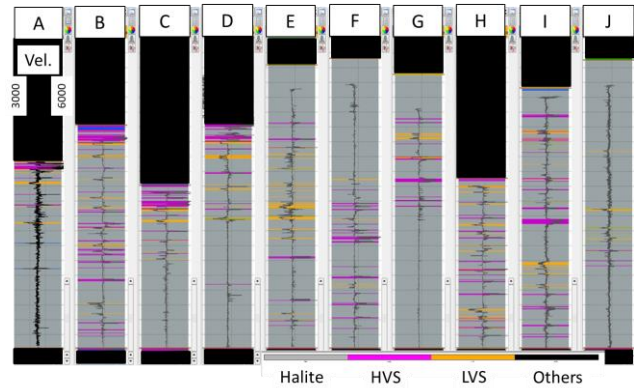


Figure 01: *Facies profile superimposed on P velocity. We can observe a good correlation between the velocity measured by sonic and the facies described during well drilling.*

The well-to-seismic tying aims to position the observed facies in their corresponding seismic event. In addition, it serves to verify the data phase shift, estimate a wavelet for inversion, AVO studies, seismic modeling (White *et al.*, 1998). After filtering the curves to a frequency near to seismic, we calculated the reflectivity function and then convolved with a wavelet resulting into the synthetic trace. The wavelet estimation used several seismic traces around well and a time window equivalent to 360ms; the operator length was 144ms.

The seismic data consists of a 3D Kirchhoff prestack depth migration (PSDM). Tomographic iterations updated the velocity model inside the Ariri Formation over an initial one, which consider almost constant velocity, equal to 4.500 m/s.

The 3D salts characterization counted with the use of seismic, attributes and velocity model. From the amplitude data, we interpreted the top and base of evaporitic section.

Results

Analyzing the facies profiles (figure 01), halite corresponds to the predominant class with 89% of the total (figure 2). HVS appears with 7% (most of the samples being anhydrite) and LVS with just 4% (carnalite corresponds to 3.8% and tachyhydrite with less of 0.2%). Sylvite occurs as an insignificant proportion and we did not quantified it.

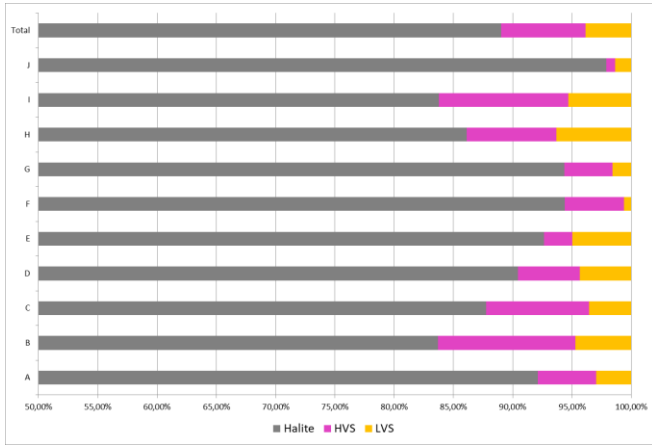


Figure 02: Salt proportion for each well. We can observe proportions differences between wells, however the sum of HVS and LVS does not exceed 20% in any of them.

Considering all the facies we estimated an average velocity of 4565 m/s with ~250 m/s of standard deviation (figure 03). This value were close to halite (4530 ± 90 m / s), fact attributed to this mineral predominance in the Ariri Formation. The HVS velocities values were 5350 ± 470 m/s and LVS were 4195 ± 295 m/s.

As we can see in the histogram of figure 3, the velocity dispersion of halite is smaller when compared to HVS and LVS. This velocity dispersion can be attributed to three factors: facies description errors, anisotropy and mineral mixtures. Cornelius and Castagna (2018) faced the same problem and concluded that mixing effect between minerals resulted in the velocities dispersions.

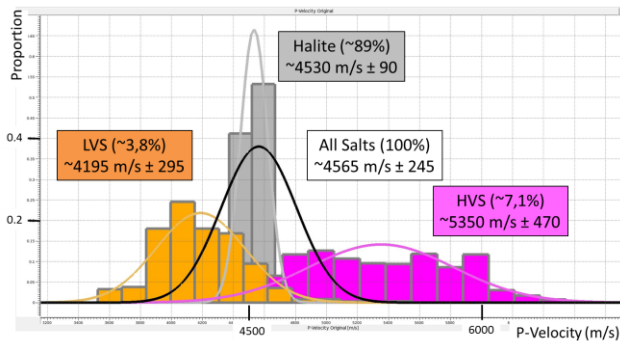


Figure 3: The salt velocities distributions in the studied area. Observe the dispersion values of HVS and LVS, this can be attributed to the mixing effect between minerals.

In regions with no P-sonic information (figure 04, first track), we completed the curve by assigning the mean velocity value estimated in the previous stage to its respective facies. For the regions above the Ariri Formation, we extracted pseudo-logs from the P velocities modelled at the well positions.

We edited and completed the density and S-velocities curves using the P-wave and facies information. Through the relations between the P-velocity and others information, we estimate regressions that better adjusted the properties (figure 05). For S-velocity, an equation third degree resulted in a correlation of 0.91, between the regression curve and property values. In terms of density, the regressions reached a poor correlation and due this, we calculated an equation for each group of salt. For the post salt region, we simply applied the Gardner (1974) relation to obtain the density curve. For the S-velocity, we used the Castagna (1985) equation. We can see the completed curves results in figure 06.

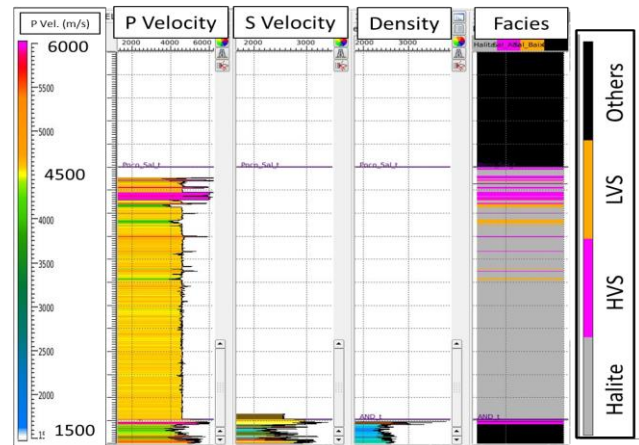


Figure 04: Original curves of well A. In this case only the P sonic was logged.

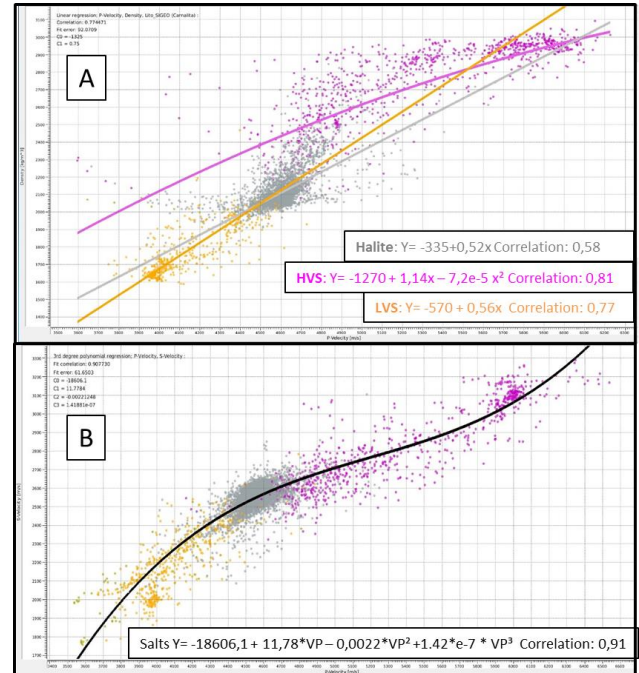


Figure 5: Estimated regressions for P velocity versus Density (figure A) and P velocity versus S velocity (figure B).

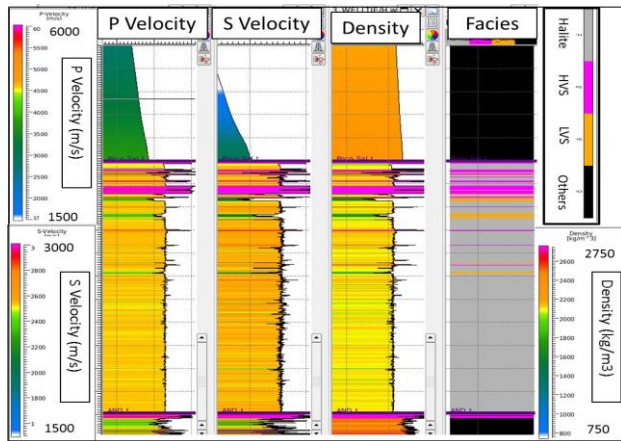


Figure 06: Well logs completed by the relationships applied on this study.

From seismic data, it is possible to recognize different features in the Ariri Formation interval. There were portions of intense alternation of positive and negative reflections and regions without impedance contrast. We associated positive reflections with presence of HVS and negative reflections generally with LVS. An anhydrite with thickness between 10-50m marks the top and base of Ariri Formation.

In this work, the seismic facies studies were based on the classification proposed by Maul *et al.* (2018). In the mentioned study, the authors recognized four seismic facies, based on behavior of seismic reflections and facies present in wells (figure 07).

- 1) Stratified seismic facies: regions with intense alternation of reflections resulting from the acoustic impedance contrast between different layers.
- 2) Chaotic seismic facies: areas where seismic reflections are disturbed, inclined and banded.
- 3) Homogeneous seismic facies: regions without reflections on the seismic data.
- 4) Hidden seismic facies: areas where we do not recognize any reflection, however the seismic response is not imaged due to seismic resolution, incidence angle, dip of salt layers.

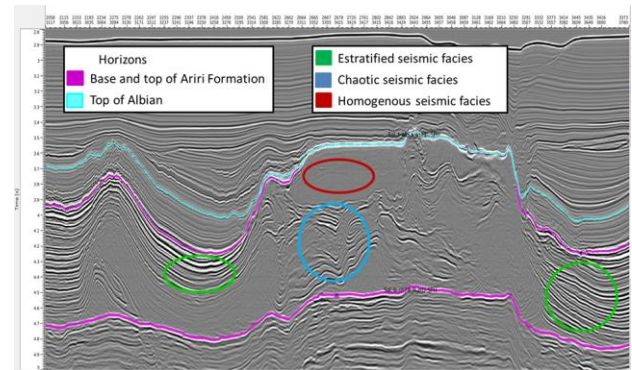


Figure 07: Seismic section with the interpreted horizons. The colored circles represents the seismic facies diagnosed on this study.

The seismic data shows a high signal noise ratio and peak frequency around 30 Hz, above 80 Hz (figure 08) practically we do not have any seismic information. Using the 1/4 of wavelength criterion (Widess 1973, Kallweit & Wood 1982), the seismic resolution is around 37.5 m.

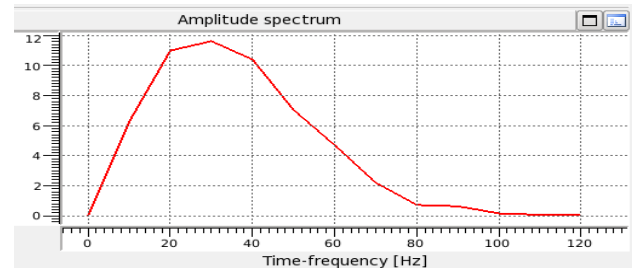


Figure 08: Amplitude spectrum of seismic data. The peak frequency is around 30 Hz and there is a lack of information over 80 Hz.

The velocity model (Fig. 09) has a low frequency content, around 4 Hz, consequently the vertical resolution is lower than seismic. The average velocity of this model is 4,500 m/s, value close to halite. Due to the poor resolution, we did not use the velocity model for salt distributions studies.

The energy envelope attribute (figure 10) represents the instantaneous energy of the signal and is proportional in its magnitude to the reflection coefficient, thus indicating regions with properties contrast. With this attribute, we can distinguish regions without reflections (homogeneous seismic facies) of areas with salt stratifications (stratified and chaotic seismic facies).

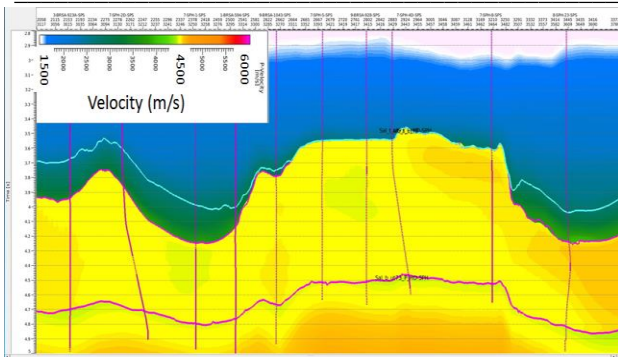


Figure 09: Tomographic velocity model used in the seismic migration. Note the low variability of the velocity values.

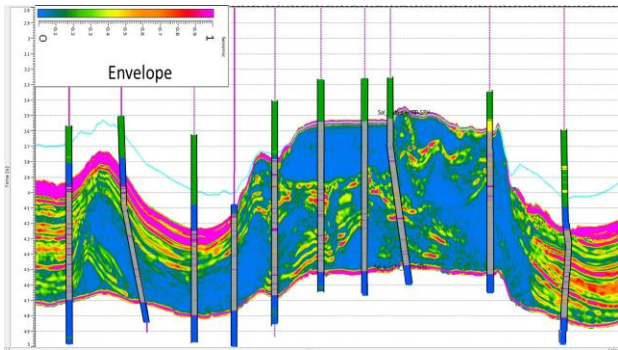


Figure 10: Section showing the energy envelope attribute. Regions with reflections have high envelope values and areas without reflectors have low envelope values.

Analyzing salt thickness map with the RMS (root mean square) amplitude attribute, we have that regions where the salt layer is thick the RMS amplitude value is low and vice-versa (figure 11). The RMS as well the envelope can only separate the stratified seismic facies from the homogeneous areas.

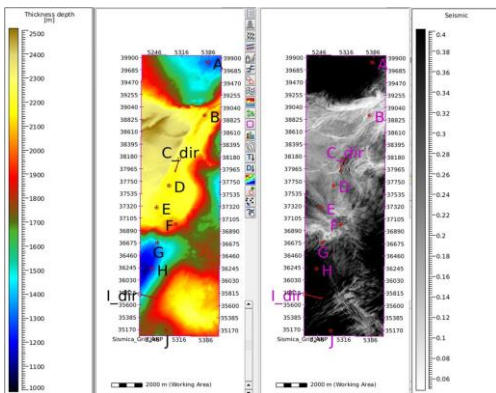


Figure 11: Thickness map (right) and RMS amplitude map (left) calculated within evaporite section. High RMS values identify stratified regions.

The well ties occurred in the fullstack time seismic, using both the edited and original curves (figures 12 and 13).

Before tying, we upscale the logs information (frequency around kHz) to a value close to seismic (~30Hz). This is an important fact to mention, because measurements on a specific scale generally behave differently at another frequency.

Both the edited and original curves resulted in correlation coefficients about 0.80 with seismic traces. This high correlation results from a good quality of amplitude data and reflects that geological features present in the evaporitic section, which were registered by the seismic images.

The seismic facies analyzed in amplitude data are correlated with salts recognized in wells. In regions with homogeneous seismic facies, there was a halite predominance, while in stratified and chaotic zones of halites intercalated with HVS and LVS. However, in some regions, we verified side lobe effect associated with anhydrite presence (strong positive amplitude associated with two negatives lobes).

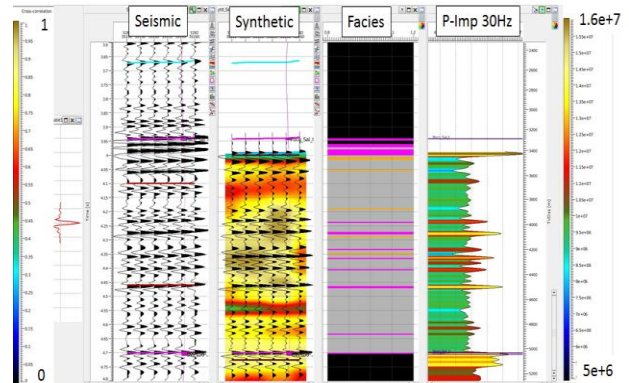


Figure 12: Well tie using the original curves.

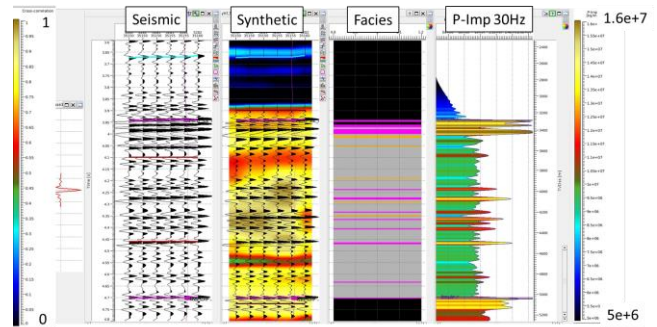


Figure 13: Well tie using the edited curves.

Conclusions

The Ariri Formation, in the studied area, has a high complexity, observable in well and the seismic scale. About 90% of the salts are composed of halite, 6% by HVS and 4% by LVS. The average evaporite velocity was 4565 m/s, halite 4530 m/s, HVS 5350 m/s and LVS 4177 m/s

Analyzing the seismic data is possible to recognize three kind of seismic facies: homogeneous, stratified and chaotic. Through the velocity model, it was not possible to distinguish the salts, but with the energy envelope

attribute, it is possible to discern zones with intercalations of facies of the non-intercalations.

The tied wells in zone without reflections in seismic data exhibit a low correlation coefficient between the synthetic and seismic, whereas in stratified zones had a high correlation.

Acknowledgments

The authors would like to thank the ANP for providing the data (Protocol nº 089525/2018 of 07/05/2018), Petrobras for the use of the software and UFF for the quality of the postgraduate program.

References

- Amaral, P.J.T., Maul, A.R., Falcão, L., Cruz, N.M.S, Gonzalez, M.A. and González, G., (2015) Estudo Estatístico da Velocidade dos Sais na Camada Evaporítica na Bacia de Santos. 14th International Congress of the Brazilian Geophysical Society & EXPOGEF, Rio de Janeiro, Brazil, 3-6 August 2015: pp. 666-669. <https://doi.org/10.1190/sbgf2015-131>
- Castagna, J. P.; Batzle, M. L. and Eastwood, R. L. (1985). Relationships between compressional-wave and shear-wave velocities in clastic silicate rocks. *Geophysics*. 50: 571–581. doi:10.1190/1.1441933.
- Cornelius, S., and Castagna, J.P., 2018. Variation in salt-body interval velocities in the deepwater Gulf of Mexico: Keathley Canyon and Walker Ridge areas. *Interpretation*, 6(1), T15-T27. <https://doi.org/10.1190/INT-2017-0069.1>
- Crain, E. M., 2015, *Crain Petrophysical Handbook* (<http://www.spec2000.net>)
- Kallweit, R. and Wood, L., 1982. The limits of resolution of zero-phase wavelets: 618 *Geophysics*, v. 47, no. 7, p. 1035-1046. <https://doi.org/10.1190/1.1441367>
- Gambôa, L., Machado, M., Silveira, De Freitas, J. and Da Silva, S., 2008, Evaporitos estratificados no Atlântico Sul: Interpretação sísmica e controle tectono-estratigráfico na Bacia de Santos, in Mohriak, W., *et al.*, eds., *Sal: Geologia e Tectônica, Exemplos nas Bacias Brasileiras*: São Paulo, Brasil, Beca Edições Ltd., p. 340–359.
- Gardner, G.H.F.; Gardner L.W. and Gregory A.R. (1974). Formation velocity and density -- the diagnostic basics for stratigraphic traps. *Geophysics*. 39: 770–780. doi:10.1190/1.1440465.
- Maul, A., Santos, A. and Silva, C., 2018. Few Considerations, Warnings and Benefits for the E&P Industry when Incorporating Stratifications Inside Salt Section. *Revista Brasileira de Geofísica*, [S.l.], v. 36, n. 4, p. 1-18, dez. 2018. ISSN 1809-4511. <http://dx.doi.org/10.22564/rbfg.v36i4.1981>
- Mavko G., Mukerji T. and Dvorkin J., 2009, *Rock Physics Handbook*, Cambridge
- Sonnenfeld, P. 1984. *Brines and Evaporites*. Academic Press. 613p.
- White, R.E., Simm, R. and Xu, S., 2008. Well tie, fluid substitution and AVO modelling – a North Sea example: *Geophysical Prospecting* 46, 323–346.
- Widess, M., 1973. How thin is a thin bed?: *Geophysics*, v. 38, no. 6, p. 1176-1180.
- Yamamoto, T., Maul, A., Born, E., Gobatto, F., Campos, M. T. and González, M., 2016. Incorporação de Estratificações Salíferas na Modelagem de Velocidade de uma Jazida da Bacia de Santos. VII Simpósio Brasileiro de Geofísica, Ouro Preto – MG